

# A New Pathway for Heterogenisation of Molecular Catalysts by Non-covalent Interactions with Carbon Nanoreactors

Maria A. Lebedeva<sup>a</sup>, Thomas W. Chamberlain<sup>a</sup>, Martin Schröder<sup>a</sup> and Andrei N. Khlobystov<sup>\*a,b</sup>.

<sup>a</sup>*School of Chemistry, University of Nottingham, Nottingham, NG7 2RD, UK*

<sup>b</sup>*Nottingham Nanotechnology and Nanoscience Centre, University of Nottingham, University Park, Nottingham, NG7 2RD, UK.*

Email: Andrei N. Khlobystov; andrei.khlobystov@nottingham.ac.uk

## Abstract

A novel approach to heterogenisation of catalytic molecules is demonstrated using the nanoscale graphitic step-edges inside hollow graphitised carbon nanofibres (GNFs). The presence of the fullerene C<sub>60</sub> moiety within a fullerene-salen Cu<sup>II</sup> complex is essential for anchoring the catalyst within the GNF nanoreactor as demonstrated by comparison with the analogous catalyst complex without the fullerene group. The presence of the catalyst at the step-edges of the GNFs is confirmed by high resolution transmission electron microscopy (TEM) and energy dispersive X-ray spectroscopy (EDX) with UV/Vis spectroscopy demonstrating only negligible (*c.a.* 3 %) desorption of the fullerene-salen Cu<sup>II</sup> complex from the GNFs into solution under typical reaction conditions. The catalyst immobilised in GNFs shows good catalytic activity and selectivity towards styrene epoxidation, comparable to the analogous catalyst in solution. Moreover, the fullerene-salen Cu<sup>II</sup> complex in GNFs demonstrates excellent stability and recyclability as it can be readily separated from the reaction mixture and employed in multiple reaction cycles with minimal loss of activity, which is highly advantageous compared to catalysts not stabilised by the graphitic step-edges that desorb rapidly from GNFs.

## Introduction

The ability to separate and recycle the metal catalyst from reaction mixtures without excessive purification steps is crucial for sustainable transition-metal based catalysis.<sup>[1]</sup> Recyclability of catalysts can be enhanced by heterogenisation of the catalyst molecules,

achieved by immobilisation on solid supports. This improves the stability of the molecular catalyst and moreover renders it insoluble in commonly used organic solvents thus offering a straightforward separation of the catalyst from the reaction mixture.<sup>[2]</sup> Heterogenisation of a molecular catalyst can be achieved by immobilisation on a variety of supports using covalent or non-covalent binding between the catalyst molecules and the support material. The preparation of covalently linked catalysts can be synthetically very demanding, requiring the preparation of non-symmetric ligands bearing functional groups that can form chemical bonds with the support material.<sup>[3]</sup> On the other hand, non-covalent immobilisation can in principle be achieved more readily, and results in the formation of materials in which the structure and the intrinsic properties of the molecular catalyst are retained. Non-covalent catalyst binding has been achieved in a variety of ways including immobilisation of catalysts on organic and inorganic supports such as polystyrenes and other polymers,<sup>[4]</sup> silica,<sup>[5]</sup> mesoporous materials<sup>[6]</sup> and zeolites,<sup>[7]</sup> by trapping the catalyst molecules inside porous hosts,<sup>[8]</sup> and *via* formation of hydrogen bonds, metal coordination<sup>[9]</sup> or electrostatic interactions<sup>[10]</sup> between the catalyst molecule and the support material.

Non-covalent heterogenisation of molecular catalysts also presents several important challenges. Non-covalent interactions are usually reversible resulting in the gradual loss of the catalytic activity upon recycling.<sup>[11]</sup> Hence a good anchoring group is required to provide sufficient binding of the catalyst to the surface of the support to afford high stability of the resulting heterogeneous material. Additionally, non-covalent interactions often lower the degree of control over the location of the catalyst molecules on the support surface. Carbon nanostructures such as carbon nanotubes (CNT) and graphite have been used extensively as robust supporting materials for immobilisation of catalysts on both internal and external surfaces and provide excellent stability, thermal and electric conductivity. For example, extended conjugated systems of  $sp^2$ -carbons of CNT and graphite allow catalyst molecules tagged with polyaromatic hydrocarbons such as pyrene to be anchored to the surface using  $\pi$ - $\pi$  stacking interactions.<sup>[12]</sup> However such anchoring is relatively weak, low-directional and is not site specific with the catalyst deposited randomly over the carbon surface.

In this study we report a new methodology for heterogenisation of transition metal catalysts by tagging them with a fullerene group which allows reliable and site-specific anchoring inside graphitised carbon nanofibres (GNF) *via* strong van der Waals interactions between the fullerene cage and the internal graphitic step-edges of GNFs. The spherical shape and large  $\pi$ -electron system of functionalised  $C_{60}$  fullerenes is known to have a high affinity for  $sp^2$ -

hybridised carbon structures and is an excellent match for the preferential binding at graphitic step-edges rather than the flat terrace of the inner surface of the GNF support.<sup>[13]</sup> We demonstrate herein that non-covalent immobilisation of a fullerene-tagged [Cu(salen)] catalyst inside GNF nanoreactors can be used to form well-defined heterogeneous catalysts with molecules located in a very distinct, confined environment. These heterogeneous catalysts exhibit enhanced stability and recyclability, whilst retaining the activity and selectivity of the individual catalytic centres.

## Experimental Section

Compounds **1** and **2** were synthesised according to the previously reported procedures.<sup>Error! Bookmark not defined.</sup> Graphitised carbon nanofibres (PR19 Pyrograf, chemical vapour deposition) were thermally annealed at 400 °C for 30 minutes prior to use. Styrene was passed through neutral alumina shortly before all reactions. All other reagents and solvents were purchased from Sigma-Aldrich and used without further purification. Reactions were carried out under aerobic atmosphere and monitored by <sup>1</sup>H NMR spectroscopy. <sup>1</sup>H NMR spectra were recorded using Bruker DPX 300 spectrometer. UV/Vis spectra were measured using a Lambda 25 Perkin Elmer Spectrometer.

### *Preparation of heterogeneous catalyst **1**@GNF and **2**@GNF.*

GNFs (5 mg) were annealed at 400 °C for 30 minutes and immersed into a solution of the corresponding [Cu(salen)] complex (**1**, 0.2 mg, 0.16 μmol; or **2**, 0.1 mg, 0.16 μmol) in THF (2 mL). The mixture was treated by ultrasound and stirred for 30 min, and the solvent slowly removed under reduced pressure. A new portion of THF (2 mL) was added, and the procedure repeated 4 times to ensure complete encapsulation of the molecules in GNFs. Upon completion the **1**@GNF and **2**@GNF catalysts were dried under vacuum for 20 h.

### *HRTEM characterisation.*

HRTEM imaging was performed using a JEOL 2100F transmission electron microscope (field emission electron gun, information limit 0.19 nm) using an accelerating voltage of 200 kV. TEM specimens were prepared by casting several drops of a methanolic suspension of **1**@GNF or **2**@GNF onto a nickel TEM specimen grid mounted “lacey” carbon film and dried under a stream of nitrogen. EDX spectra were recorded for isolated nanofibres of **1**@GNF or **2**@GNF using an Oxford Instruments X-rays detector at 200 kV.

*Leaching test.*

**1**@GNF (5 mg, 0.16  $\mu$ mol of Cu complex) or **2**@GNF (5 mg, 0.16  $\mu$ mol of Cu complex) was immersed in MeCN (4 mL) and heated to 50 °C in a sealed UV/Vis cell, and absorption spectra of the resulting solution were measured every 10 min.

*Styrene epoxidation.*

The catalyst (**1**, 0.2 mg, 0.16  $\mu$ mol; **2**, 0.1 mg, 0.16  $\mu$ mol; **1**@GNF, 5 mg, 0.16  $\mu$ mol; **2**@GNF, 5 mg, 0.16  $\mu$ mol; or GNF, 5 mg) was dissolved or suspended in MeCN (1 mL) containing styrene (52 mg, 0.5 mmol), and a solution of <sup>t</sup>BuOOH in nonane (5.5 M, 0.27 mL, 1.5 mmol) was added. The reaction mixture was heated to 80 °C for 7 h, and aliquots of the reaction mixture were then analysed by <sup>1</sup>H NMR spectroscopy in CDCl<sub>3</sub> solution after each hour without further purification. All quoted reactions yields are a result of at least 3 repeat reactions.

Styrene, **a**: <sup>1</sup>H NMR (300 MHz, CDCl<sub>3</sub>,  $\delta$ ): 7.30-7.50 (m, 5H, Ar H), 6.69 (dd, J=17.6, 10.9 Hz; 1H, CH=CH<sub>2</sub>), 5.72 (d, J=17.6 Hz; 1H, CH=CH<sub>2</sub>), 5.22 (d, J=10.9 Hz; 1H, CH=CH<sub>2</sub>).

Styrene epoxide, **b**: <sup>1</sup>H NMR (300 MHz, CDCl<sub>3</sub>,  $\delta$ ): 7.30-7.50 (m, 5H, Ar H), 3.86 (m, 1H, -CH(O)-), 3.15 (dd, J=5.5, 4.1 Hz; 1H, CH(O)-CH<sub>2</sub>), 2.80 (dd, J=5.5, 2.6 Hz; 1H, CH(O)-CH<sub>2</sub>).

**c**: <sup>1</sup>H NMR (300 MHz, CDCl<sub>3</sub>,  $\delta$ ): 7.20-7.40 (m, 5H, Ar H), 5.28 (dd, J=8.0, 3.6 Hz; 1H), 4.08-4.24 (m, 2H).

**d**: <sup>1</sup>H NMR (300 MHz, CDCl<sub>3</sub>,  $\delta$ ): 7.20-7.40 (m, 5H, Ar H), 5.03 (d, J=7.7 Hz; 1H), 4.08-4.24 (m, 2H).

**e**: <sup>1</sup>H NMR (300 MHz, CDCl<sub>3</sub>,  $\delta$ ): 10.02 (s, 1H, CH=O), 7.20-7.40 (m, 5H, Ar H), 5.09 (s, 2H).

*Leaching test under catalytic conditions.*

The catalyst (**1**@GNF, 2.5 mg, 0.08  $\mu$ mol or **2**@GNF, 2.5 mg, 0.08  $\mu$ mol) was suspended in MeCN (0.5 mL) containing styrene (26 mg, 0.25 mmol), and in some cases solution of <sup>t</sup>BuOOH in nonane (5.5 M, 0.13 mL, 1.5 mmol) was added. The reaction mixture was heated

to 80 °C for 7 h, and filtered hot to remove the insoluble materials. The filtrate was then diluted to 5 mL and analysed using UV/Vis spectroscopy.

#### *Recyclability test.*

Styrene epoxidation was performed as described above. After heating the reaction mixture to 80 °C for 7 h the reaction mixture was allowed to cool to room temperature, the catalyst was removed by filtration, washed extensively with cold CH<sub>3</sub>CN (20 mL) and dried under vacuum for 20 h. The resulting material was then used in the next catalytic cycle.

### **Results and Discussion**

Transition metal complexes of salen derivatives are established as highly successful and versatile catalysts. The scope of reactions catalysed by metal-salen complexes is extremely wide and includes carbon-carbon bond formation, heteroatom-heteroatom bond formation and carbon-heteroatom bond formation reactions.<sup>[14]</sup> We have synthesised the fullerene-tagged Cu(II) salen complex **1** (Figure 1) in six steps according to our recently reported procedure.<sup>[15]</sup> The analogous fullerene-free complex **2** was prepared for comparison. [Cu(II)(salen)] complexes are known to catalyse epoxidation reactions of alkenes, and it has been demonstrated previously that a slight enhancement of the catalytic activity of the transition metal complex is observed upon addition of the fullerene cage due to the electron withdrawing nature of the carbon cage.<sup>[15]</sup>

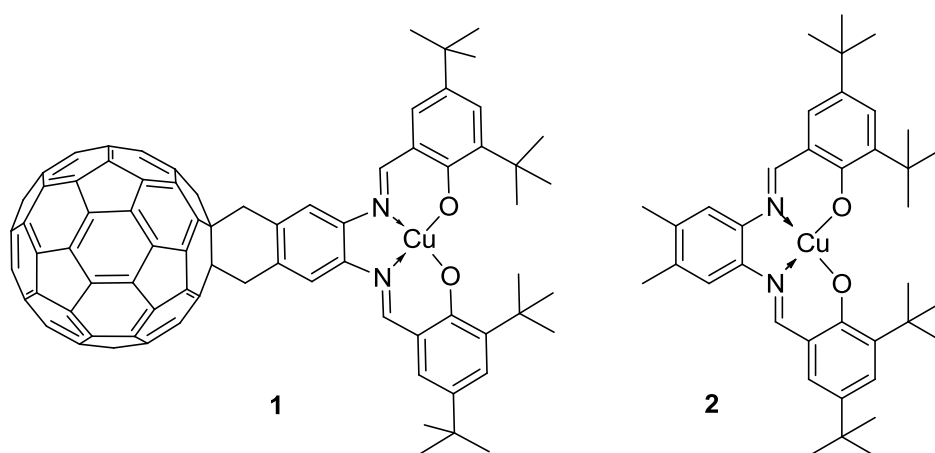


**Figure 1.** Structure of the fullerene derivatised [Cu(salen)] complex (**1**) and its fullerene-free analogue (**2**).

Immobilisation and encapsulation of fullerene-containing molecules inside single-, double- and multi-walled carbon nanotubes has been extensively studied and the procedure to achieve

high filling yields is now well-established.<sup>[16]</sup> In contrast, GNF have not been used widely for fullerene encapsulation due to their very wide internal diameters (50-70 nm). However, the structure of GNF consists of stacked truncated cones of graphite layers and this creates sequence of step-edges (Figure 2a) which are ideally suited to accommodate catalyst molecules. Indeed, it has been demonstrated previously for various metal nanoparticles that guest species are located predominantly on these step-edge sites.<sup>[17,18,19]</sup> Furthermore, the diameters of GNFs are sufficiently large to minimise diffusion resistance of the reactant and product molecules to and from the catalytic centres.

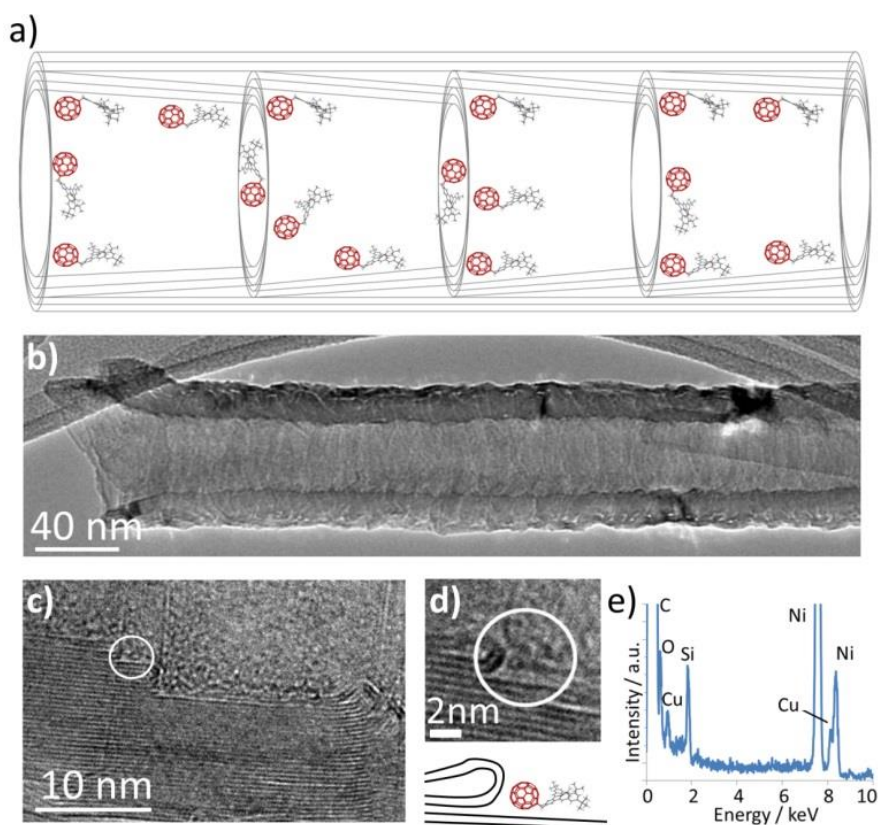


**Figure 2.** a) Schematic representation of **1**@GNF showing fullerene-containing molecules located preferentially on the step-edges of the GNF (fullerene molecules and GNF are not drawn to scale). TEM images of **1**@GNF show b) the accessible internal channel of the nanoreactor, c) the internal surface of a GNF filled with **1** (white circle) and d) a high-magnification TEM image of **1**@GNF showing an individual molecule of **1** located on the step-edge of the GNF (top) and its schematic representation (bottom). e) EDX spectroscopy confirms the presence of copper within the **1**@GNF structure (the Ni peaks are due to the TEM specimen grid).

The heterogeneous catalyst, **1**@GNF, was prepared by introducing the fullerene-tagged molecules into the internal channel of GNF using a solution method. Initially the GNFs were thermally treated at 400 °C to remove any residual water molecules from their internal channels and then immersed into a saturated solution of **1** in THF followed by slow removal of the solvent under reduced pressure to deposit the molecules onto the GNF. Fresh solvent was then added to dissolve any molecules on the outside surface of the GNF, and this procedure was repeated several times to ensure a high degree of pore filling. Immobilisation of control compound **2** into GNF was carried out using the same method. The structures of the resultant composite materials (**1**@GNF and **2**@GNF respectively, Figure 2a) were analysed by high-resolution transmission electron microscopy (HR-TEM, Figure 2 b, c). HR-TEM images of **1**@GNF show the presence of the individual fullerene containing molecules (Figure 2c, observed as circles with diameter of *c.a.* 0.7 nm) located on the internal step-edges of the GNF so that the surface of contact between the C<sub>60</sub> moiety and the step-edge of GNF is maximised (Figure 2d). The presence of the [Cu(salen)] moiety is more difficult to visualise as the majority of organic molecules rapidly decompose under the electron beam of TEM. However, the presence of copper inside the GNF was confirmed by localised energy dispersive x-ray (EDX) spectroscopy (Figure 2e). The structure of **2**@GNF was also analysed by HR-TEM and although fullerene-free molecules were not resolved in the micrograph, the presence of the copper containing species was also confirmed by EDX.

This procedure enables deposition of the molecules predominantly on the inside of the GNF, and also enables precise control of the total amount of catalyst loaded into the GNF support. The catalyst loading in both **1**@GNF and **2**@GNF was 0.03 mmol of copper salen catalyst per gram of GNF which is comparable to similar immobilised metal catalysts in CNTs attached using either covalent<sup>[20,21,22]</sup> or non-covalent bonding.<sup>[23,24]</sup> Table S1 compares the catalyst loading in the present study with systems reported previously. The efficiency of the catalyst immobilisation in GNFs was quantified by comparing the amount of catalyst which leached from the GNFs into solution over time (Figure 3). The same amount of freshly prepared **1**@GNF or **2**@GNF with identical catalyst loading was immersed in an excess of MeCN and heated to 50 °C in a sealed vessel. The resulting solution was analysed by UV/Vis spectroscopy over time (Figure 3). The majority of the fullerene containing molecules (97%) was retained in the GNF giving an almost colourless solution (Figure 3, inset (left)). In comparison, the fullerene-free complex **2** rapidly leached from the GNF support to form a bright-yellow solution (Figure 3, inset (right)) with only 30% of the initial complex retained

in the GNF after 5 h. This confirms that attachment of the fullerene cage to the active [Cu(salen)] catalyst has a dramatic effect on host-guest interactions within the pores of the support and consequently the stability of the resulting composite materials.

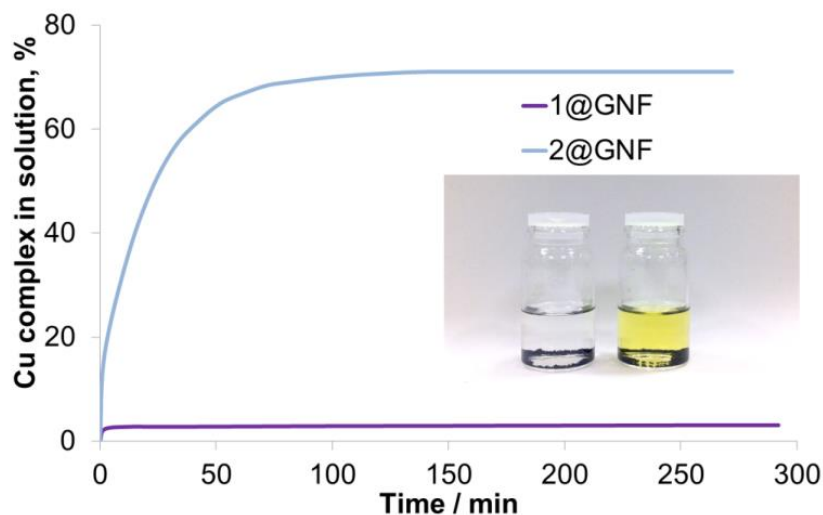
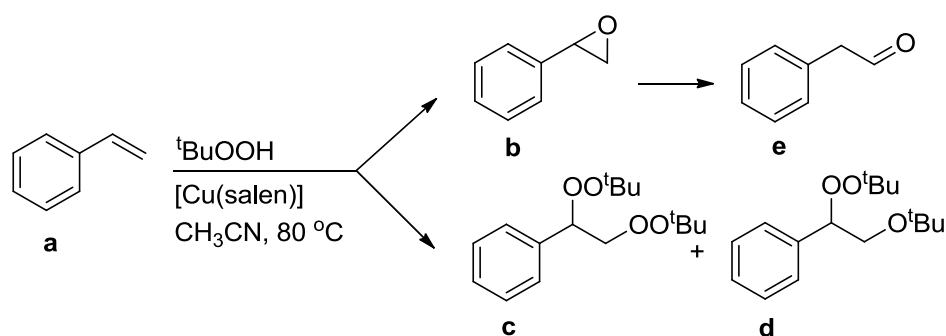


**Figure 3.** Plot showing the amount of the metal complex leached into MeCN at 50 °C over time for **1**@GNF (purple line) and **2**@GNF (blue line); inset shows photographs of the resultant mixtures of **1**@GNF (left) and **2**@GNF in MeCN (right) after 5 h.

The performance of the heterogeneous catalysts **1**@GNF and **2**@GNF was compared in a model styrene epoxidation reaction along with the molecules **1** and **2** under homogeneous conditions (Scheme 1 and Table 1). Styrene was reacted with <sup>t</sup>BuOOH in dry MeCN at 80 °C under an aerobic atmosphere, and the reaction mixture was monitored over time by <sup>1</sup>H NMR spectroscopy. The reaction gives a distribution of four different products (Scheme 1), with the target epoxide, **b**, undergoing further transformations to form the corresponding aldehyde **e**, and radical addition products **c** and **d**. The formation of epoxide is promoted by Cu<sup>II</sup> centres *via* formation of a Cu<sup>III</sup> peroxo metalocycle intermediate which then breaks to yield the styrene oxide and regenerate the Cu<sup>II</sup> complex.<sup>25</sup>





**Scheme 1.** Epoxidation of styrene (**a**) by <sup>t</sup>BuOOH in the presence of [Cu(salen)] forming styrene epoxide (**b**), 1-phenyl-1,2-bis-*tert*-butylperoxy ether (**c**), 1-phenyl-1-*tert*-butylperoxy-2-*tert*-butyloxy ether (**d**) and 2-phenylacetaldehyde (**e**).

**Table 1.** Catalytic epoxidation of styrene with <sup>t</sup>BuOOH in MeCN at 80 °C showing the distribution of compounds **a-e** after 7 h.

Catalyst	Yield [%]				
	<b>a</b>	<b>b</b>	<b>c</b>	<b>d</b>	<b>E</b>
<b>1</b>	0	46 ± 2	15 ± 2	29 ± 2	10 ± 2
<b>2</b>	0	42 ± 2	26 ± 2	20 ± 2	12 ± 1
<b>1</b> @GNF	0	42 ± 2	19 ± 2	29 ± 2	10 ± 1
<b>2</b> @GNF	0	43 ± 1	14 ± 1	31 ± 2	12 ± 1
GNF	16 ± 2	8 ± 1	50 ± 2	22 ± 2	4 ± 0.5
No catalyst	46 ± 3	2 ± 0.5	39 ± 2	12 ± 1	1 ± 0.5

Indeed, in the absence of catalyst only 2 % of styrene epoxide is formed (Scheme 1, compound **b**; Table 1), and the major products are compounds **c** (39 %) and **d** (12 %) (Scheme 1) formed as a result of an undesirable radical addition of *tert*-butyl peroxide radicals to the double bond of styrene.<sup>26</sup> In the presence of empty GNFs a similar trend is observed in which the epoxide **b** is a minor product (8 % yield) and formation of compounds **c** and **d** is favoured (50 and 22 % respectively). Introducing catalysts **1** or **2** promotes epoxide formation preferentially forming product **b** (42-46 %) rather than **c** (15-26 %) and **d** (29-20 %). This activity and selectivity is comparable with the majority of catalytic systems reported before for styrene epoxidation (see Table S2). The formation of **e**, which is a product of rearrangement of epoxide **b**, depends on the amount of epoxide in the reaction mixture. However, it is always a minor product and the total yield of **e** only reaches a maximum of ~10 %. The yield and the rate of the reaction catalysed by fullerene-containing complex **1** is slightly higher than the reaction catalysed by fullerene-free complex **2** (green and orange curves respectively in Figure 4). This is the result of the electron withdrawing effect of the fullerene cage depleting the electron density on the Cu<sup>II</sup> centre and promoting its catalytic activity, consistent with previous observations.<sup>15</sup>

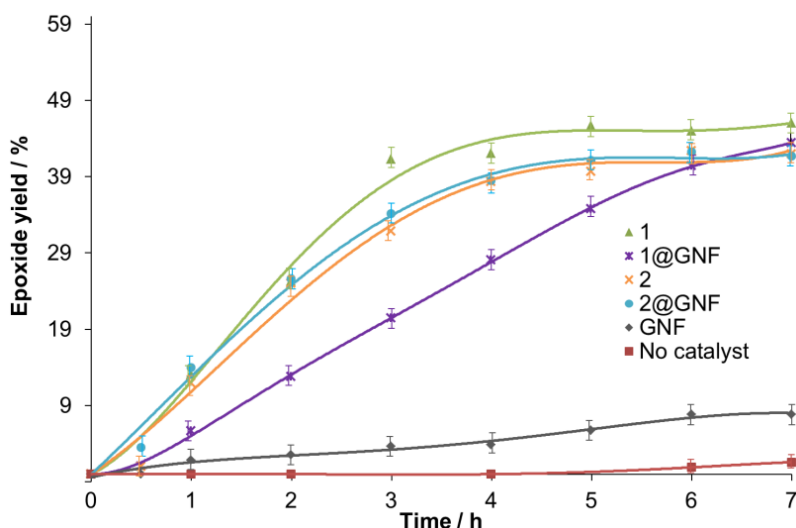


**Figure 4.** Rate of formation of styrene epoxide from styrene in the presence of **1** (green), **2** (orange), **1@GNF** (purple), **2@GNF** (blue), GNF (grey) and in the absence of catalyst (red line).

Complete conversion of styrene, **a**, and a 42 % yield of epoxide, **b**, is achieved in the presence of the heterogeneous catalyst **1@GNF** in 7 h, an outcome very similar to the homogeneous reaction. The heterogeneously catalysed reaction however, occurs noticeably slower than the reaction in solution (Figure 4, purple and green curves respectively). This is attributed to fact that the catalytic centres are less accessible in **1@GNF** due to the confinement inside the GNF nanoreactor. As a result, complete conversion of styrene and formation of similar amounts of styrene epoxide are achieved over a slightly longer period as compared to the solution reaction (Figure 4). This difference in the reaction rates of **1** and **1@GNF** also confirms that the catalyst molecules remain immobilised on the GNF throughout the whole process under these conditions. In comparison, under the same reaction conditions **2@GNF** shows a nearly identical rate of formation of styrene epoxide to **2** in solution (Figure 4, orange and blue curves respectively), indicating that both reactions occur in solution under homogeneous conditions. Similar trends are observed for the kinetic curves for styrene conversion and for selectivity for styrene epoxide monitored over time (Figures S2 and S3).

These trends are further supported by the UV/Vis spectroscopy measurements of the reaction mixtures under catalytic conditions. Leaching tests were carried out in the absence of <sup>t</sup>BuOOH to simplify quantitative measurements (see SI for details), but in otherwise identical conditions to the catalytic reaction, and these confirm that the majority of the catalyst is

leached out of **2**@GNF into solution as a result of only weak interactions between **2** and the GNF. In contrast, 97 % of molecules of **1** are retained on GNF (Figure S5 and Table S3).

To highlight the excellent stability of this heterogeneous catalytic system formed using non-covalent interactions between the fullerene-tagged **1** and GNF, we studied the recyclability of **1**@GNF over a number of repeat catalytic cycles. We tested the performance of **1**@GNF and **2**@GNF in five consecutive epoxidation reactions of styrene (Figure 5) with each cycle lasting 7 h. The catalyst was separated from the reaction mixture after each cycle by filtration, extensively washed with MeCN to remove any traces of the reactants/products and utilised in the next otherwise identical reaction cycle. The conversion of styrene was 100 % for all catalytic cycles. An identical 42% yield of epoxide was achieved for both catalysts in the first cycles of catalysis. However, the catalytic activity of **2**@GNF shows a significant drop in the second cycle forming only 27% of styrene epoxide (Figure 5, blue columns) whereas the fullerene-containing **1**@GNF affords a 37% yield of styrene epoxide (Figure 5, purple columns). Further decrease in activity is observed for **2**@GNF showing only 22% yield of epoxide after 5 cycles, whereas in the presence of **1**@GNF even after 5 cycles the yield of epoxide remains significantly higher and stabilises at 34% yield. These results confirm the excellent stability of **1**@GNF in which the catalytic centres are retained on the support material for longer. In addition, spatial separation of the fullerene-tagged metal complex on the GNF step-edges may also prevent decomposition of the catalyst molecules which can occur in solution due to both epoxidation/polymerisation of the fullerene cage and dimerization of the [Cu(salen)] complex leading to the formation of inactive dimeric species and aggregates<sup>27</sup> under aerobic atmosphere at elevated temperature.

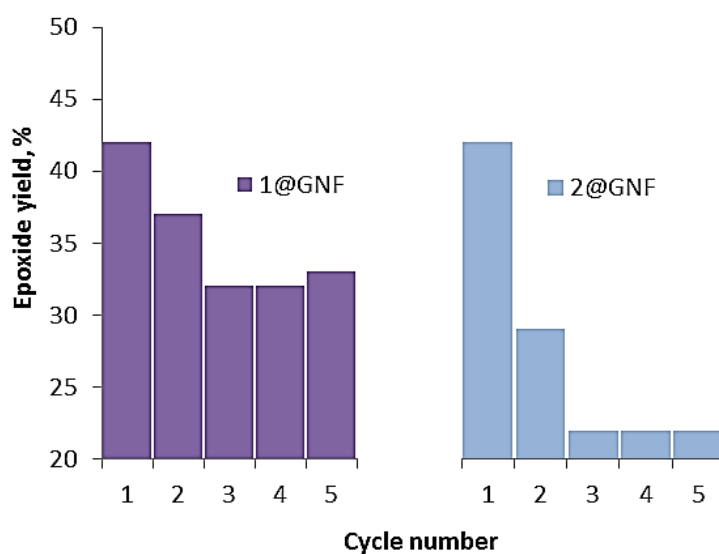


**Figure 5.** Comparison of the stability and recyclability of the catalyst in **1**@GNF (purple) and **2**@GNF (blue) in five consecutive epoxidation reaction cycles of styrene of 7 h.

## Conclusions

A non-covalent supramolecular approach for the heterogenisation of molecular catalysts has been developed utilising the unique affinity of C<sub>60</sub> fullerene for carbon nanostructures. A fullerene-tagged [Cu(salen)] complex has been incorporated into GNFs to form robust and stable catalytically active nanostructures. Fullerene-GNF interactions are sufficiently strong to allow the catalyst molecules to be retained in the GNFs when heated in MeCN over many hours. As a result this material possesses excellent recyclability while showing a significantly better activity compared to a catalyst without fullerene over multiple reaction cycles.

Synthetic methodologies to tag a variety of transition metal complexes with a fullerene cage<sup>28</sup> including various bipyridine,<sup>29</sup> terpyridine<sup>30</sup> and porphyrin<sup>31</sup> complexes have been extensively developed in the past decade enabling our methodology to be expanded to a variety of other existing catalytic systems. The enhanced catalyst recyclability achieved in GNFs can be particularly valuable for processes involving rare metals such as Ru, Os, Pd, Pt, Ag and Au and has the potential to significantly lower the cost of their usage in industrial processes.

## Supporting Information Available

Additional <sup>1</sup>H NMR spectra, UV/Vis absorption spectra, styrene epoxidation kinetic curves and additional literature data. This information is available free of charge via the Internet at <http://pubs.acs.org/>.

## Acknowledgements

This work was supported by European Research Council (ERC) (Consolidator Grant to ANK and Advanced Grant to MS), Engineering and Physical Sciences Research Council (EPSRC), and University of Nottingham.

## References

- [<sup>1</sup>] Corma, A.; Garcia, H. *Chem. Rev.* **2002**, *102*, 3837.
- [<sup>2</sup>] Baleizão, C.; Garcia, H. *Chem. Rev.* **2006**, *106*, 3987.

- [<sup>3</sup>] (a) Kim, J. H.; Kim, G. J. *Catal. Lett.* **2004**, *92*, 123; (b) Park, D. W.; Choi, S. D.; Choi, S. J.; Lee, C. Y.; Kim, G. J. *Catal. Lett.* **2002**, *78*, 145.
- [<sup>4</sup>] Lu, J.; Toy, P. *Chem. Rev.* **2009**, *109*, 815.
- [<sup>5</sup>] (a) Choudary, B.; Ramani, T.; Maheswaran, H.; Prashant, L.; Ranganath, K.; Kumar, K. *Adv. Synth. Catal.* **2006**, *348*, 493; (b) Kantam, M.; Ramani, T.; Chakrapani, L.; Choudary, B. *J. Mol. Catal. A.: Chem.* **2007**, *274*, 11.
- [<sup>6</sup>] Serrano, D.; Aguado, J.; Vargas, C. *App. Catal., A* **2008**, *335*, 172.
- [<sup>7</sup>] Guo, X.-F.; Kim, Y.-S.; Kim, G.-J. *Top. Catal.* **2009**, *52*, 153.
- [<sup>8</sup>] Corma, A.; Garcia, H. *Eur. J. Inorg. Chem.* **2004**, 1143.
- [<sup>9</sup>] Baleizao, C.; Gigante, B.; Sabater, M. J.; Garcia, H.; Corma, A. *Appl. Catal., A* **2002**, *228*, 279.
- [<sup>10</sup>] Bhattacharjee, S.; Anderson, J.A. *Chem. Commun.* **2004**, 554.
- [<sup>11</sup>] (a) Das, P.; Silva, A. R.; Carvalho, A. P.; Pires, J.; Freire, C. *Colloids Surf. A* **2008**, *329*, 190; (b) Bai, R.; Fu, X.; Bao, H.; Ren, W. *Catal. Commun.* **2008**, *9*, 1588; (c) Ren, W.; Fu, X.; Bao, H.; Bai, R.; Ding, P.; Sui, B. *Catal. Commun.* **2009**, *10*, 788; (d) Gong, B.; Fu, X.; Chen, J.; Li, Y.; Zou, X.; Tu, X.; Ding, P.; Ma, L. *J. Catal.* **2009**, *262*, 9.
- [<sup>12</sup>] (a) Liu, G.; Wu, B.; Zhang, J.; Wang, X.; Shao, M.; Wang, J. *Inorg. Chem.* **2009**, *48*, 2383; (b) Li, F.; Zhang, B.; Li, X.; Jiang, Y.; Chen, L.; Li, Y.; Sun, L. *Angew. Chem. Int. Ed.* **2011**, *50*, 12276; (c) Xing, L.; Xie, J.-H.; Chen, Y.-S.; Wang, L.-X.; Zhou, Q.-L. *Adv. Synth. Catal.* **2008**, *350*, 1013; (d) Tran, P.; Le Goff, A.; Heidkamp, J.; Jusselme, B.; Guillet, N.; Palacin, S.; Dau, H.; Fontecave, M.; V. Artero, *Angew. Chem. Int. Ed.* **2011**, *50*, 1371; (e) Vriamont, C.; Devillers, M.; Riant, O.; Hermans, S. *Chem. Eur. J.* **2013**, *19*, 12009.
- [<sup>13</sup>] Chamberlain, T.W.; Popov, A.M.; Knizhnik, A.A.; Samoilov, G.E.; Khlobystov, A.N. *ACS Nano* **2010**, *4*, 5203.
- [<sup>14</sup>] Zulauf, A.; Mellah, M.; Hong, X.; Schulz, E. *Dalton Trans* **2010**, *39*, 6911.
- [<sup>15</sup>] Lebedeva, M.A.; Chamberlain, T.W.; Davies, E.S.; Mancel, D.; Thomas, B.E.; Suyetin, M.; Bichoutskaia, E.; Schröder, M.; Khlobystov, A.N. *Chem. Eur. J.* **2013**, *19*, 11999.
- [<sup>16</sup>] (a) Chamberlain, T.W.; Pfeiffer, R.; Peterlik, H.; Kuzmany, H.; Zerbetto, F.; Melle-Franco, M.; Staddon, L.; Champness, N.R.; Briggs, G.A.D.; Khlobystov, A.N. *Small* **2008**, *4*, 2262; (b) Chamberlain, T.W.; Camenisch, A.; Champness, N.R.; Briggs, G.A.D.; Benjamin, S.C.; Ardavan, A.; Khlobystov, A.N. *J. Am. Chem. Soc.* **2007**, *129*, 8609; (c) Gimenez-Lopez, M.C.; Chuvilin, A.; Kaiser, U.; Khlobystov, A.N. *Chem. Commun.* **2011**, *47*, 2116;

(d) Chamberlain, T.W.; Champness, N.R.; Schröder, M.; Khlobystov, A.N. *Chem. Eur. J.* **2011**, *17*, 668.

[<sup>17</sup>] La Torre, A.; Fay, M.W.; Rance, G.A.; Giménez-López, M.C.; Solomonsz, W.A.; Brown, P.D.; Khlobystov, A.N. *Small* **2012**, *8*, 1222.

[<sup>18</sup>] Solomonsz, W.A.; Rance, G.A.; Suetin, M.; La Torre, A.; Bichoutskaia, E.; Khlobystov, A.N. *Chem. Eur. J.* **2012**, *18*, 13180.

[<sup>19</sup>] La Torre, A.; Giménez-López, M.C.; Fay, M.W.; Rance, G.A.; Solomonsz, W.A.; Chamberlain, T.W.; Brown, P.D.; Khlobystov, A.N. *ACS Nano* **2012**, *6*, 2000.

[<sup>20</sup>] Baleizão, C.; Gigante, B.; Garcia, H.; Corma, A. *Tetrahedron* **2004**, *60*, 10461.

[<sup>21</sup>] Nooraeipour, M.; Moghadam, M.; Tangestaninejad, S.; Mirkhani, V.; Mohammadpoor-Baltork, I.; Iravani, N. *J. Coord. Chem.* **2012**, *65*, 226.

[<sup>22</sup>] Zakeri, M.; Moghadam, M.; Mohammadpoor-Baltork, I.; Tangestaninejad, S.; Mirkhani, V.; Khosropour, A. R. *J. Coord. Chem.* **2012**, *65*, 1144.

[<sup>23</sup>] Liu, G.; Wu, B.; Zhang, J.; Wang, X.; Shao, M.; Wang, J. *Inorg. Chem.* **2009**, *48*, 2383.

[<sup>24</sup>] Xing, L.; Xie, J.-H.; Chen, Y.-S.; Wang, L.-X.; Zhou, Q.-L. *Adv. Synth. Catal.* **2008**, *350*, 1013.

[<sup>25</sup>] Su, H.; Li, Z.; Huo, Q.; Guan, J.; Kan, Q. *RSC Adv.* **2014**, *4*, 9990.

[<sup>26</sup>] (a) Minisci, F.; Fontana, F.; Araneo, S.; Recupero, F.; Banfi, S.; Quici, S. *J. Am. Chem. Soc.* **1995**, *117*, 226; (b) Minisci, F.; Fontana, F.; Araneo, S.; Rupero, F. *J. Chem. Soc., Chem. Comm.* **1994**, 1823; (c) Bravo, A.; Bjørsvik, H.-R.; Fontana, F.; Liguori, L.; Minisci, F. *J. Org. Chem.* **1997**, *62*, 3849; (d) Yu, J.-Q.; Corey, E. *Org. Lett.* **2002**, *4*, 2727.

[<sup>27</sup>] Fraile, J. M.; Garcia, J.I.; Herrerias, C.I.; Mayoral, J.A.; Pires, E. *Chem. Soc. Rev.* **2009**, *38*, 695.

[<sup>28</sup>] Meijer, M.; van Klink, G.; van Koten, G. *Coord. Chem. Rev.* **2002**, *230*, 141.

[<sup>29</sup>] (a) Maggini, M.; Guldi, D.; Mondini, S.; Scorrano, G.; Paolucci, F.; Ceroni, P.; Roffia, S. *Chem. Eur. J.* **1998**, *4*, 1992; (b) Armaroli, N.; Accorsi, G.; Felder, D.; Nierengarten, J.-F. *Chem. Eur. J.* **2002**, *8*, 2314; (c) Zhou, Z.; Sarova, G.; Zhang, S.; Ou, Z.; Tat, F.; Kadish, K.; Echegoyen, Guldi, D.; Schuster, D.; Wilson, S. *Chem. Eur. J.* **2006**, *12*, 4241.

[<sup>30</sup>] (a) Fu, K.; Henbest, K.; Zhang, Y.; Valentin, S.; Sun, Y.-P. *J. Photochem. and Photobiol. A: Chem.* **2002**, *150*, 143; (b) Gao, Y.; Song, Y.; Li, Y.; Wang, Y.; Liu, H.; Zhu, D. *Appl. Phys. B* **2003**, *76*, 761.

[<sup>31</sup>] (a) Song, L.-C.; Liu, X.-F.; Xie, Z.-J.; Luo, F.-X.; Song, H.-B. *Inorg. Chem.* **2011**, *50*, 11162; (b) Xu, W.; Feng, L.; Wu, Y.; Wang, T.; Wu, J.; Xiang, J.; Li, B.; Jiang, L.; Shu, C.; Wang, C. *Phys. Chem. Chem. Phys.* **2011**, *13*, 428; (c) D'Souza, F.; Gadde, S.; Islam, S.; Wijesinghe, C.; Schumacher, A.; Zandler, M.; Araki, Y.; Ito, O. *J. Phys. Chem. A* **2007**, *111*, 8552; (d) Vail, S.; Krawczuk, P.; Guldi, D.; Palkar, A.; Echegoyen, L.; Tomé, J.; Fazio, M.; Schuster, D. *Chem. Eur. J.*, **2005**, *11*, 3375; (e) Wijesinghe, C.; El-Khouly, M.; Zandler, M.; Fukuzumi, S.; D'Souza, F. *Chem. Eur. J.* **2013**, *19*, 9629.

## Table of contents graphic

